CHAPTER IV
RESULTS AND DISCUSSION

4.1 Formation of Microemulsion

4.1.1 Phase Behavior of Microemulsion

Figure 4.1 shows the phase behavior of microemulsion system of AOT/n-heptane/$TiCl_4$/NaCl with the weight ratio of oil to aqueous phase equals 1 at 30°C. By increasing the concentration of NaCl from 0.1 to 4.0 wt%, the phase changes from microemulsion type I (oil-in-water) to type III (bicontinuous) and finally to type II (water-in-oil) as shown in the figure.

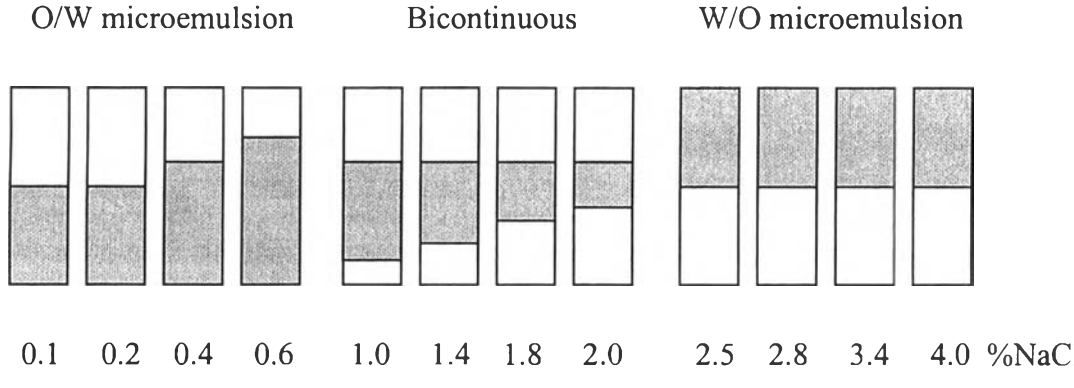

Figure 4.1 Phase behavior with salinity scan.

Increasing the electrolyte concentration decreases the ionic atmosphere surrounding the ionic head groups and consequently decreases the electrical repulsion between the charged groups within the micellar structure or increases lyophilicity in the surfactant structure, thus increases the solubilization of oil in the o/w microemulsion as it is seen by the increase of the volume of the surfactant phase. Further increasing NaCl, the middle surfactant phase was obtained because the electrical repulsion between the charged group within the micellar structure was further decreased (the entropic effect begins to dominate) and thus

decreases solubilization of water. It is seen by the separation of water phase. Eventually, at high electrolyte concentration, the electrical repulsion has much less effect than the entropy effect on the micellar structure and the surfactant favors the oil phase. It is seen as w/o microemulsion (Bourrel and Schechter, 1988).

4.1.2 Effect of Salt Level on Micellar Size and Water Content

Figure 4.2 shows the micellar size of o/w microemulsion obtained from dynamic light scattering at different concentrations of NaCl. It can be seen that by increasing the concentration of NaCl from 0.1 to 0.6 wt%, average micelle diameter increased from 15 nm to 19 nm. The size increased significantly on approaching the bicontinuous (type III) microemulsion transition. The amount of water in the microemulsion was not determined because the micellar phase was in excessive water environment.

For bicontinuous microemulsion (type III), the micellar size and the amount of water in microemulsion phase are shown in Figures 4.3 (a) and 4.3 (b), respectively. With increasing concentration of NaCl from 1.0 to 2.0 wt%, micellar size grew from 40 nm to 80 nm while amount of water decreased from 60 to 50 wt% and suddenly decreased to 30 wt% at the transition of bicontinuous to w/o microemulsion.

The micellar sizes of w/o microemulsion are presented in Figure 4.4 (a). With increasing the concentration of NaCl starting near the bicontinuous to w/o microemulsion transition at 2.5 and continuing to 8.0 wt%, the micellar size of w/o microemulsion decreases from 40 nm to 15 nm. Droplet decreases more rapidly near the transition more than away from the transition. Water decreased with increasing salt concentration in the w/o (type II) micrremulsion.

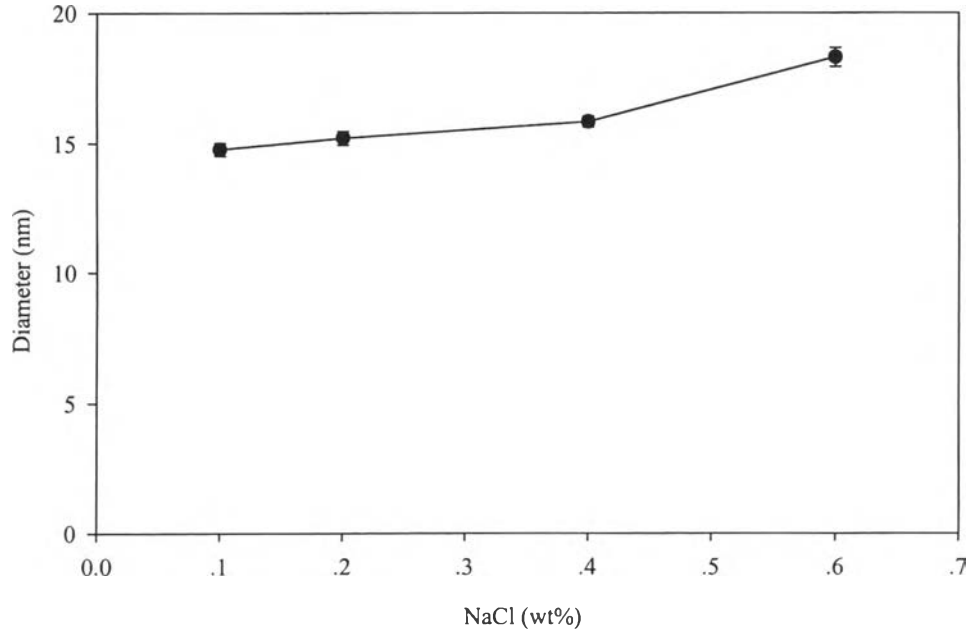

Figure 4.2 Micellar size of o/w microemulsion obtained from dynamic light scattering.

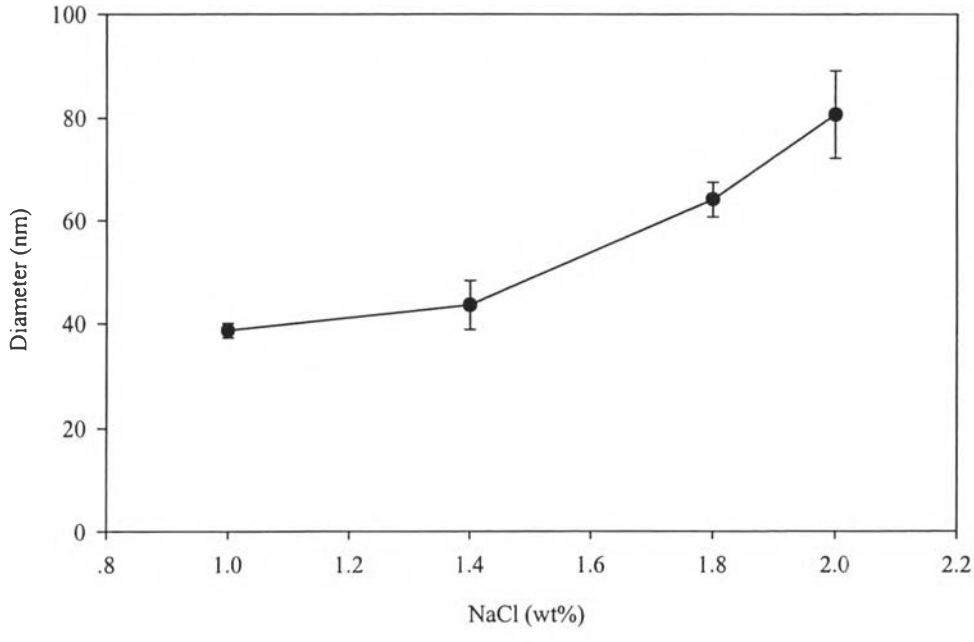

(a)

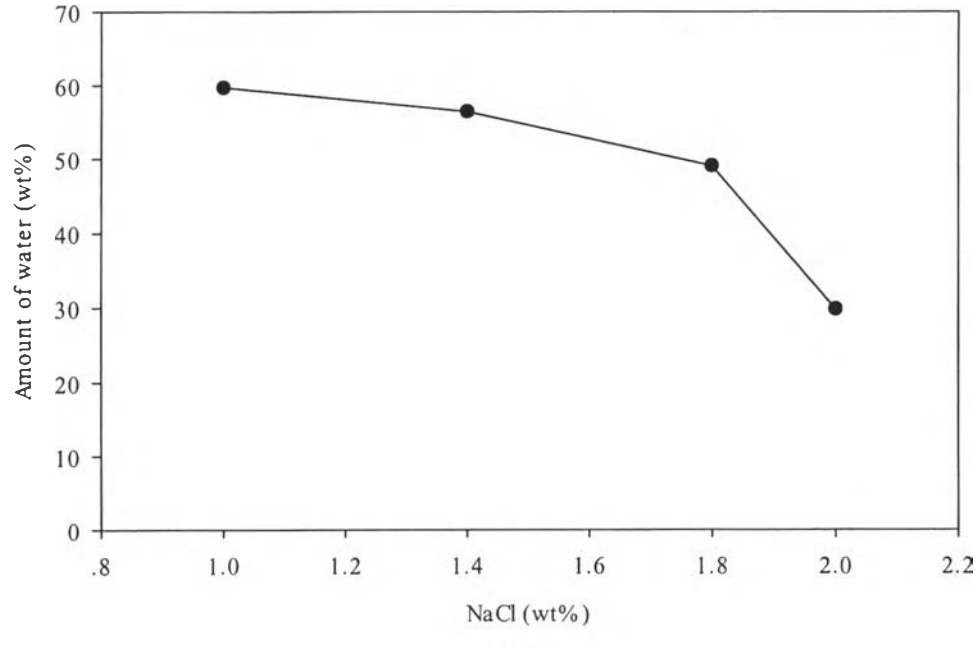

(b)

Figure 4.3 (a) Micellar size of bicontinuous microemulsion obtained from dynamic light scattering, (b) amount of water in the bicontinuous microemulsion phase.

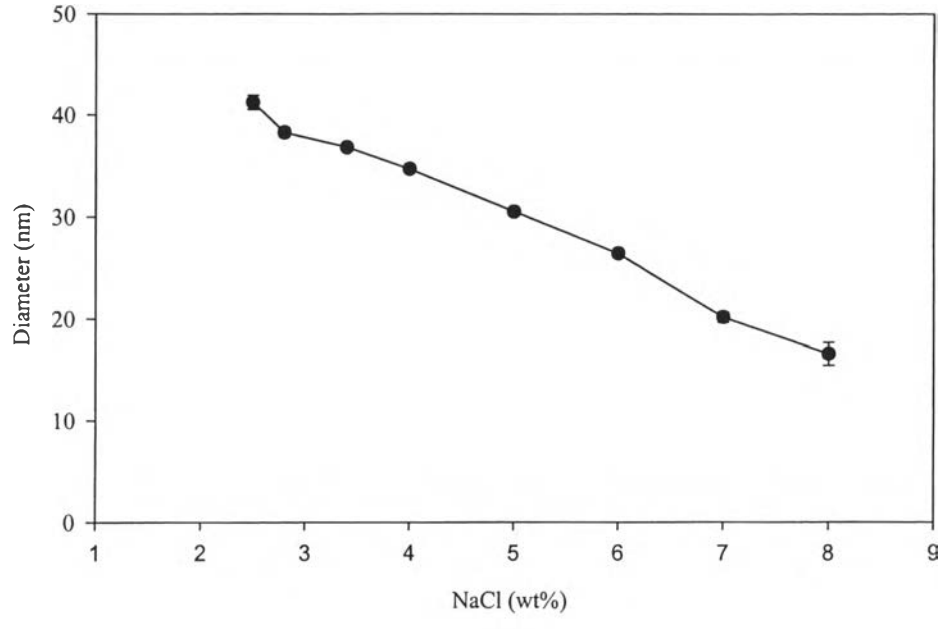

(a)

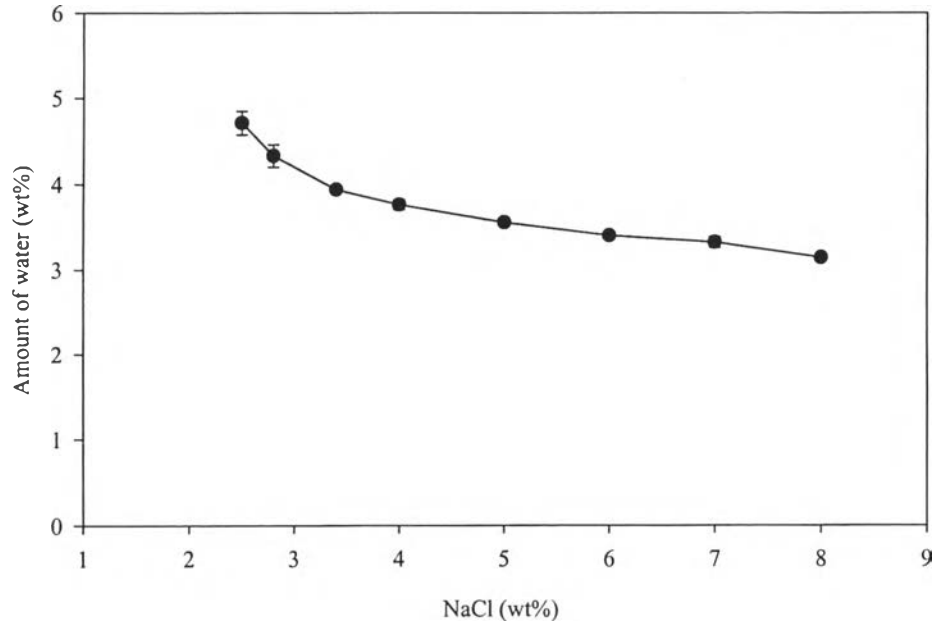

(b)

Figure 4.4 (a) Micellar size of w/o microemulsion obtained from dynamic light scattering, (b) amount of water in the w/o microemulsion phase.

4.1.3 Effects of $TiCl_4$ Concentration

Figure 4.5 shows a comparison of micellar size in o/w microemulsion at three different $TiCl_4$ concentrations and with increasing the concentration of NaCl. Dynamic light scattering indicated that the increase in the $TiCl_4$ concentration causes a decrease in the micellar size of o/w microemulsion and the most concentrated $TiCl_4$ solution gives the smallest micellar size at any given NaCl concentrations. Multivalent cation of Ti^{+4} increases the degree of binding of counter ion to the surfactant in the aqueous phase and causes a decrease in the micellar size of the surfactant.

The effect of $TiCl_4$ concentration on the micellar size and the amount of water in bicontinuous microemulsion is shown in Figure 4.6 (a) and 4.6 (b), respectively. The results show that increasing $TiCl_4$ concentration causes a decrease in the micellar size in bicontinuous microemulsion at all NaCl concentrations and it does not affect the amount of water in bicontinuous microemulsion phase.

Figure 4.7 shows the effect of $TiCl_4$ concentration on micellar size (a) and amount of water (b) for w/o microemulsion. The results show that increasing multivalent cation binding from Na^+ to Ti^{+4} decreases micellar size in w/o microemulsion. The micellar size further decreases as the concentration of Ti^{+4} increases. This effect is opposed to the change of micellar size in o/w microemulsion. Ti^{+4} ions have higher degree of binding than Na^+ ion to bind with the surfactant head group in the reverse micelle core. Increasing the multivalent ion concentration decreases the micellar size further due to a decrease in the electrical repulsion ionic head groups of micellar structure. Amount of water in w/o microemulsion shown in Figure 4.7 (b) indicates that the titanium concentration hardly affects the amount of water.

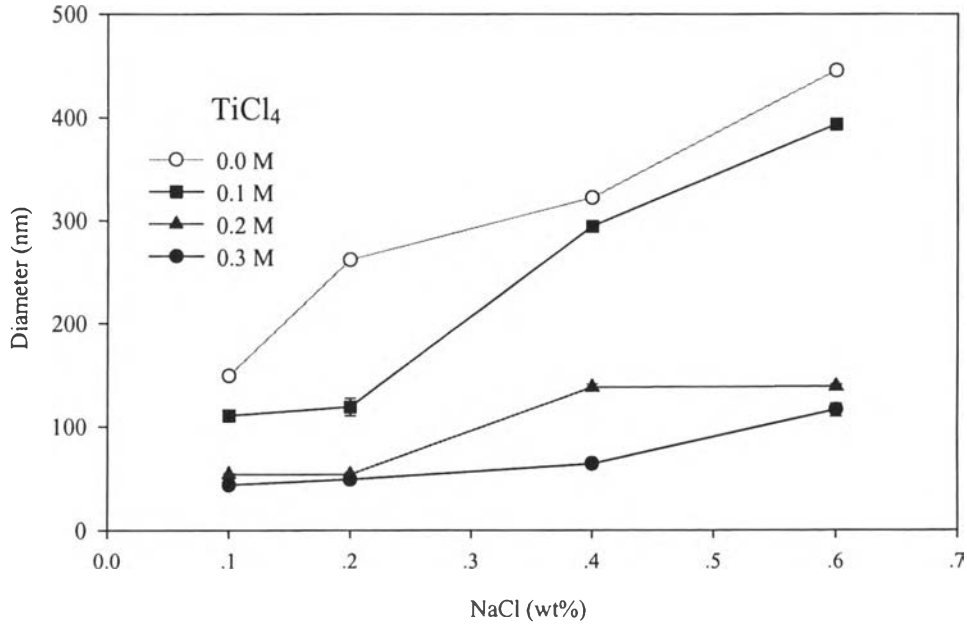

Figure 4.5 Micellar size of o/w microemulsion at different $TiCl_4$ concentrations.

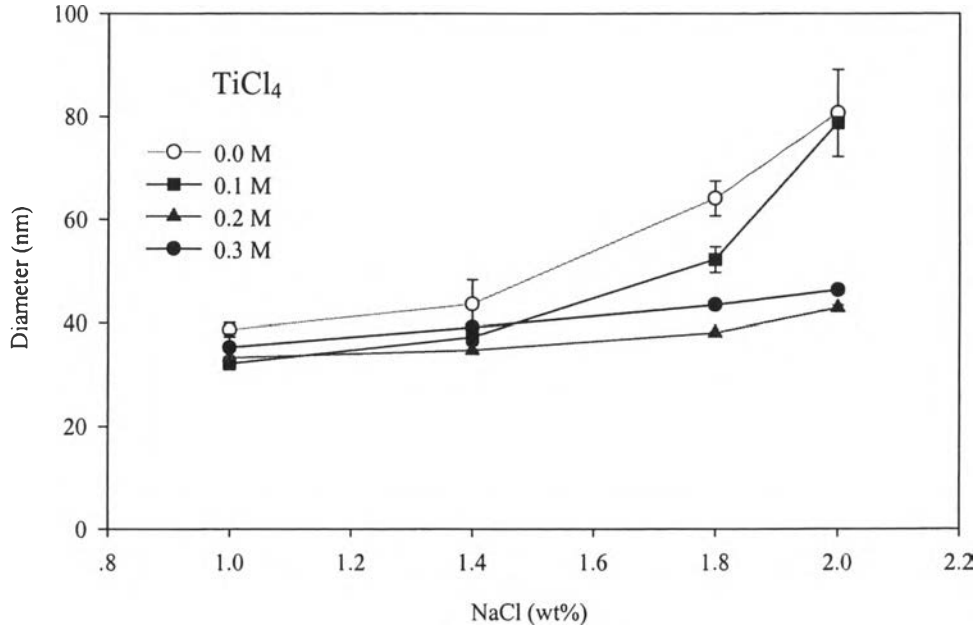

(a)

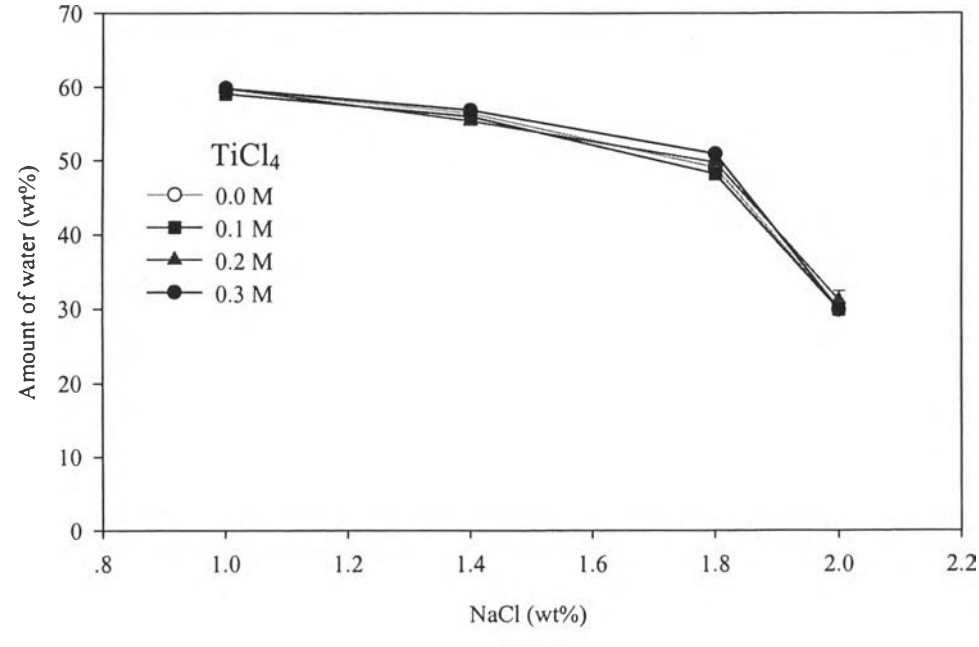

(b)

Figure 4.6 Bicontinuous microemulsion at different $TiCl_4$ concentrations (a) micellar size and (b) amount of water.

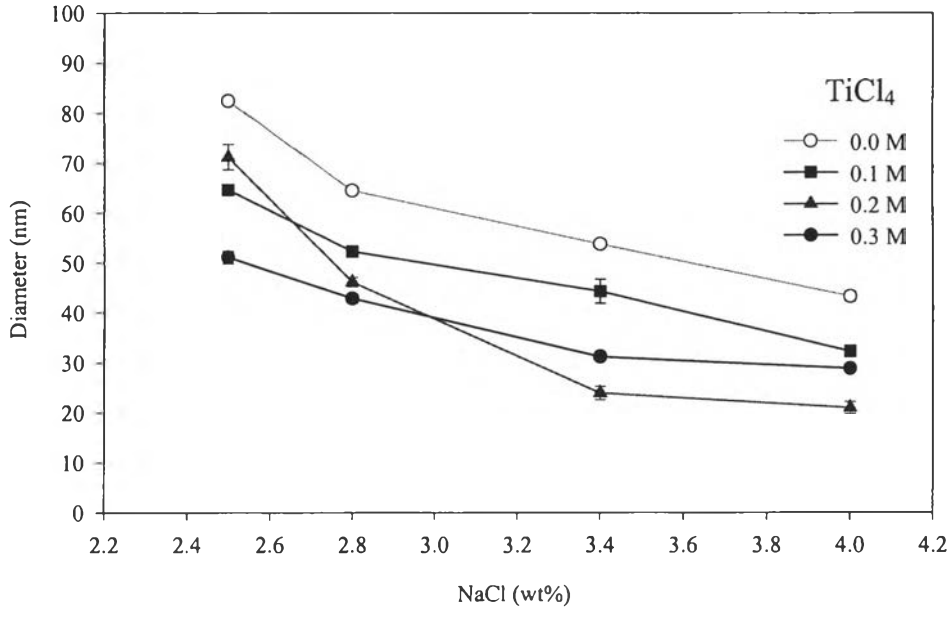

(a)

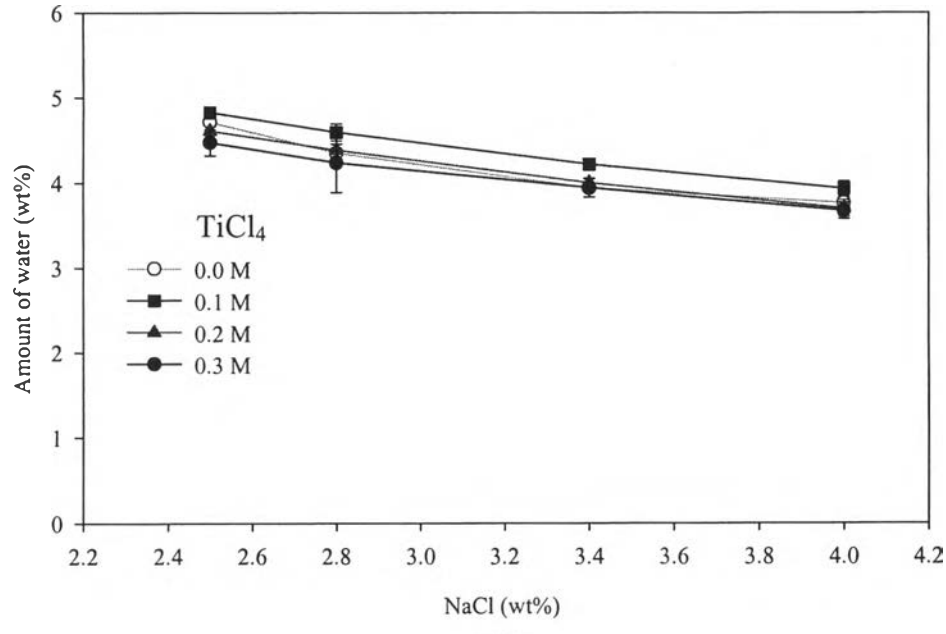

(b)

Figure 4.7 W/O microemulsion at different $TiCl_4$ concentrations (a) micellar size and (b) amount of water.

4.1.4 Effects of Weight Ratio of Oil to Aqueous Phases

Figures 4.8-4.10 show the effect of the weight ratio of oil to brine on micellar size and amount of water in three different microemulsions. At any given weight ratio of oil to brine, the micellar size in the brine phase increases for o/w and bicontinuous microemulsions, but decreases for w/o microemulsion as NaCl concentration increases. The weight ratio of oil to brine has an insignificant effect on the amount of water in all types of microemulsion.

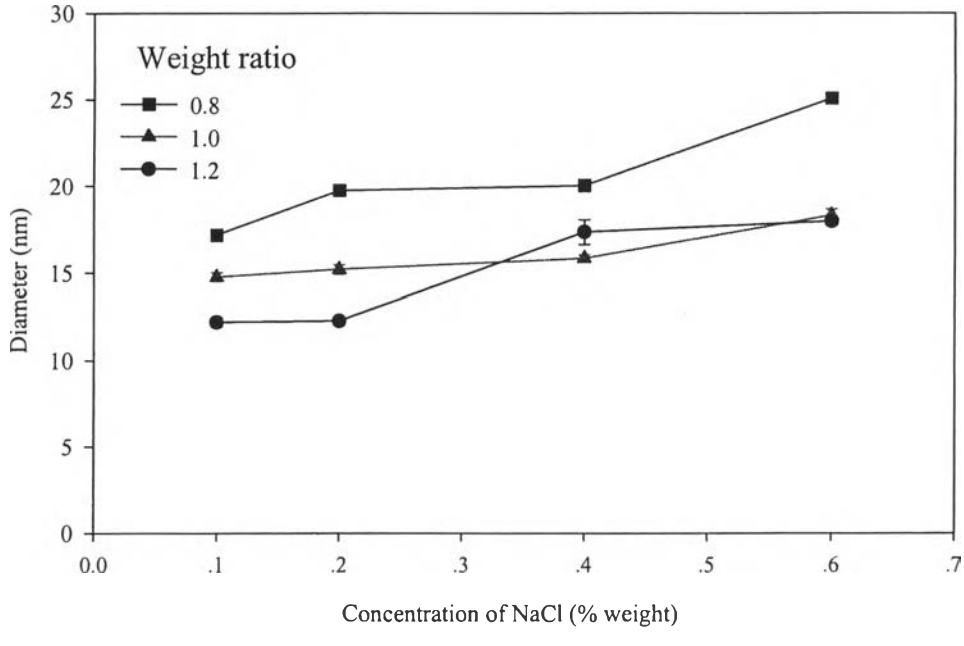

Figure 4.8 Micelle size in o/w microemulsion at different weight ratio of oil to brine phases.

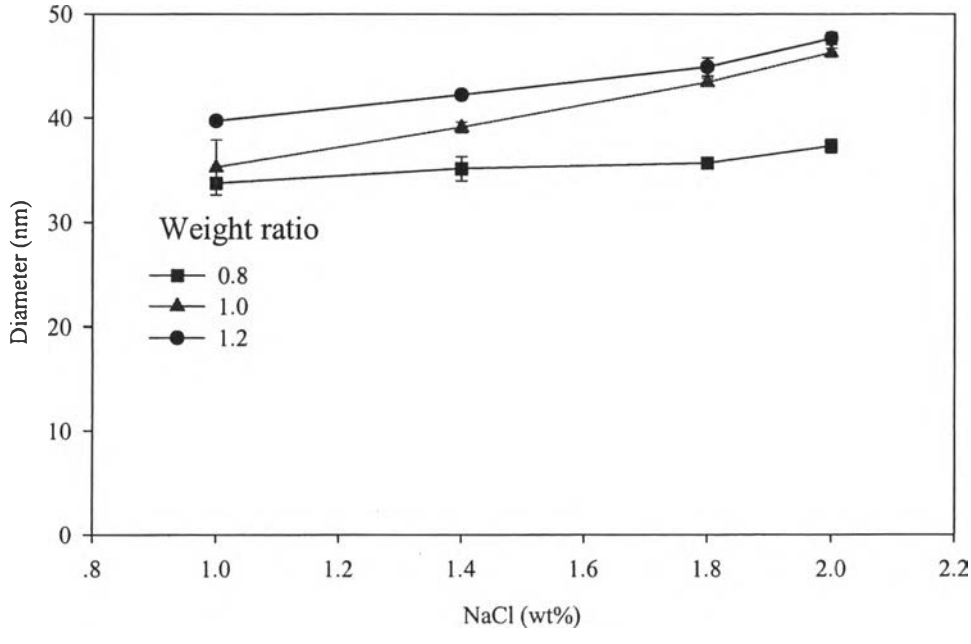

(a)

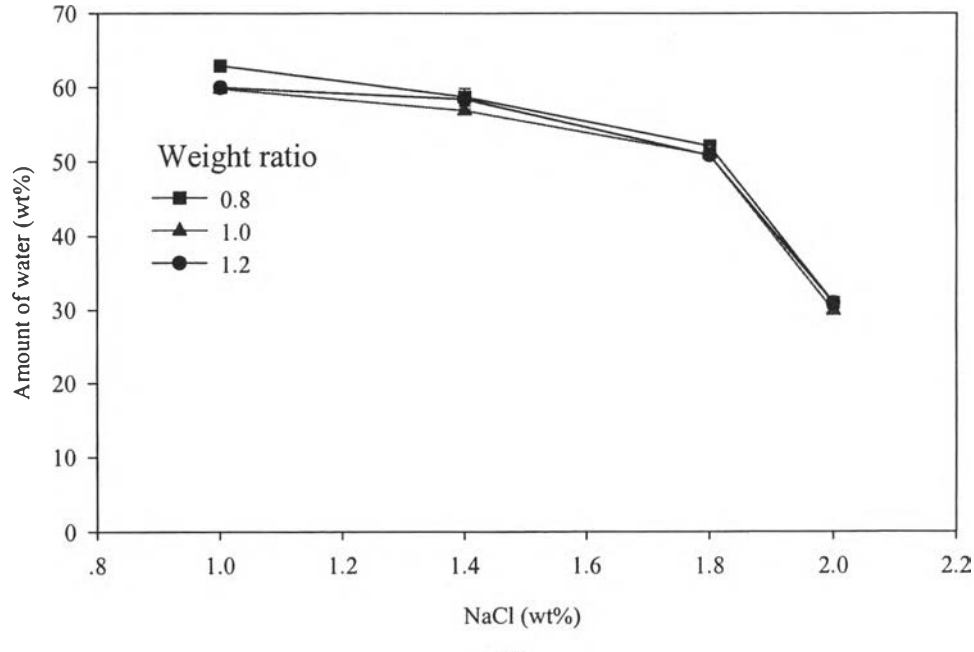

(b)

Figure 4.9 (a) Micellar size of bicontinuous microemulsion obtained from dynamic light scattering, (b) amount of water in the bicontinuous microemulsion phase.

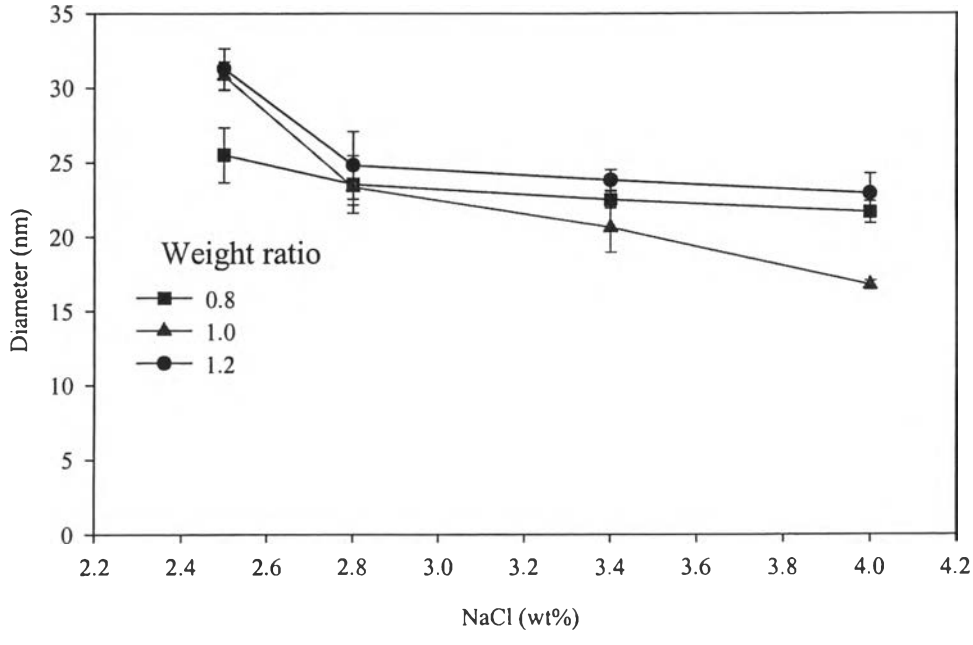

(a)

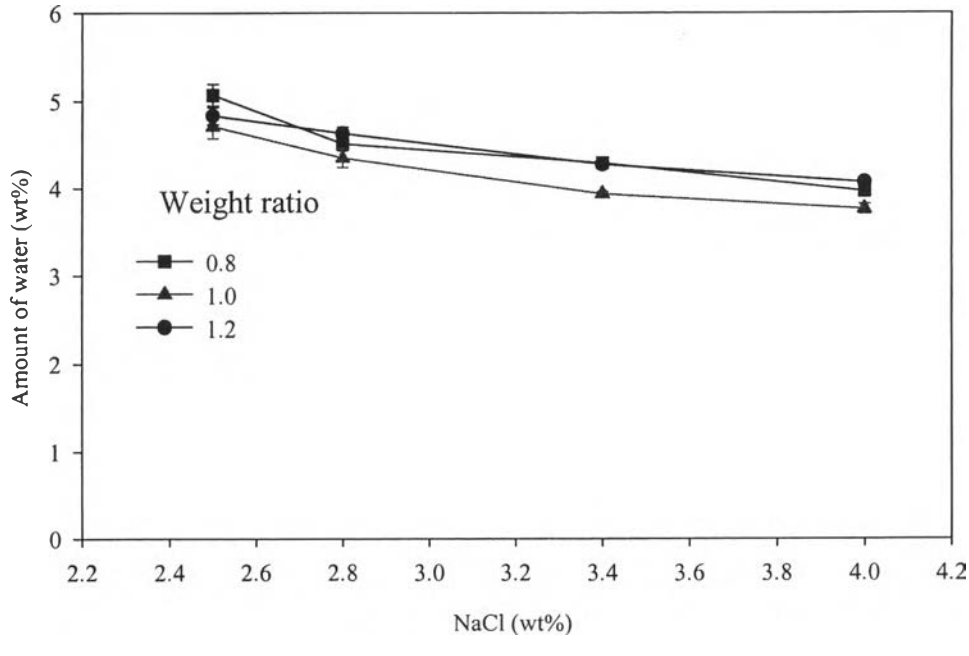

Figure 4.10 W/O Microemulsion at different weight ratio of oil to brine phases (a) micellar size and (b) amount of water.

4.2 Formation of Titanium Dioxide Particles in Microemulsion

4.2.1 Synthesis of Titanium Dioxide Particles in Microemulsions

4.2.1.1 pH studies of titanium dioxide particles

Titanium dioxide particles were obtained by introducing ammonia gas into the separated w/o microemulsion phase containing 0.3 M $TiCl_4$ and 4.0 wt% NaCl. The pH of precipitation was studied from 1.0 to 8.0 and the precipitate began to form at pH 3.0. The precipitates obtained at different pH conditions were collected, dried at 100°C for 15 hours, calcined at 500°C for 5 hours, and subjected to XRD phase analysis.

The XRD results of TiO_2 phase analysis shown in Figure 4.11 indicate that the pH does not affect the phase change of titanium dioxide at the calcinations temperature 500°C but it affects the formation of different titanium in the precipitation step. Titanium dioxide was formed at about pH 5.0-6.0 and titanium tetrahydroxide occurred at pH 8.0 and higher. It took a longer time and higher temperature to dry precipitate obtained at high pH condition.

4.2.1.2 Calcination temperature studies

The temperature for calcination was varied from 100°C to 700°C and the calcined particles were subjected to XRD analysis. The results shown in Figure 4.12 indicates that with the calcination temperature below 400°C titanium dioxide particles were amorphous, brookite near 400°C, anatase at 400-500°C, and rutile at 600°C and above. The transformation temperature depends on the nature and structure of the precursor and the preparation conditions (Chhabra *et al.*, 1995).

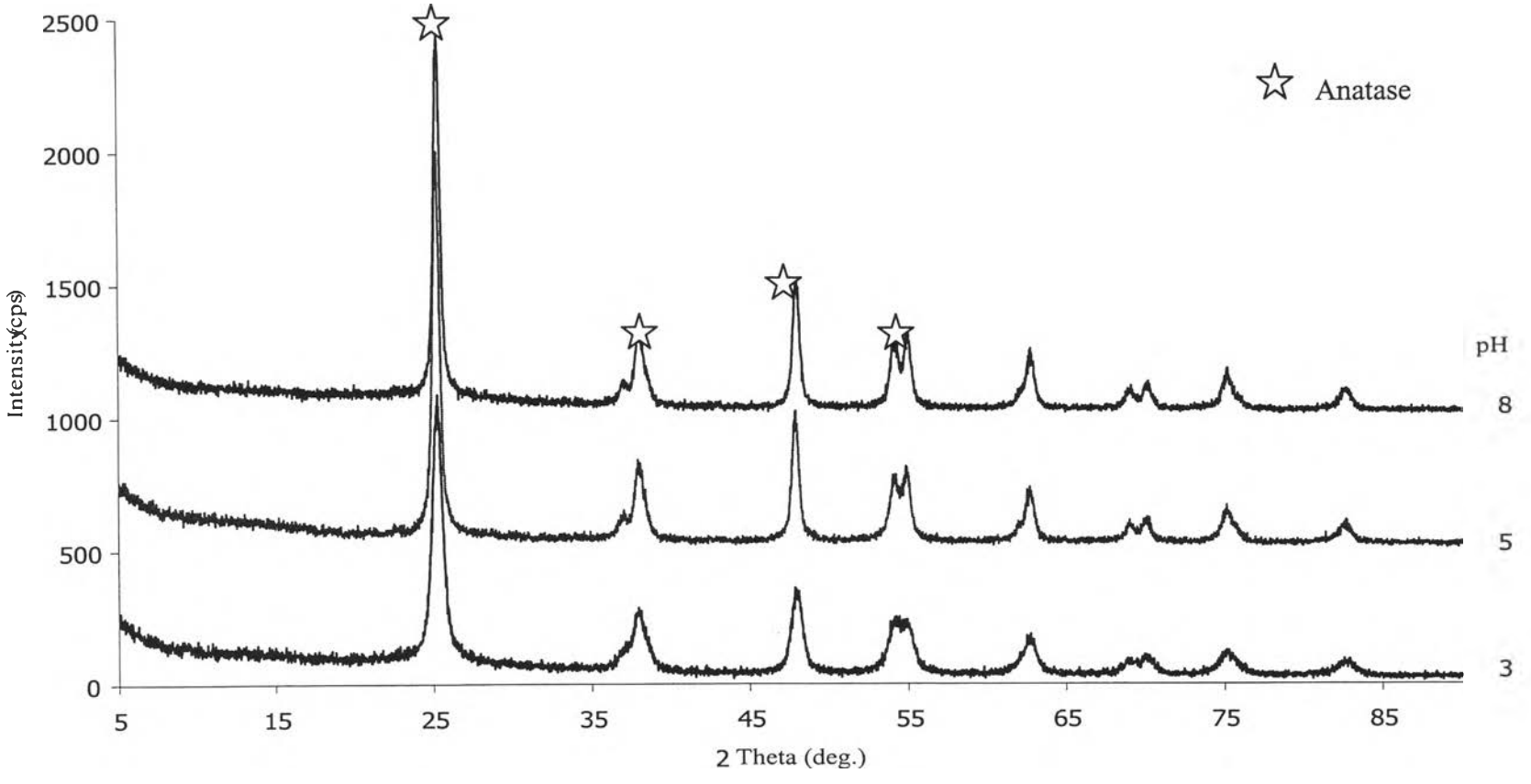

Figure 4.11 XRD patterns of titanium dioxide precipitated at different pH in w/o microemulsion containing 0.3 M $TiCl_4$ and 4.0% NaCl and calcination temperature at 500°C.

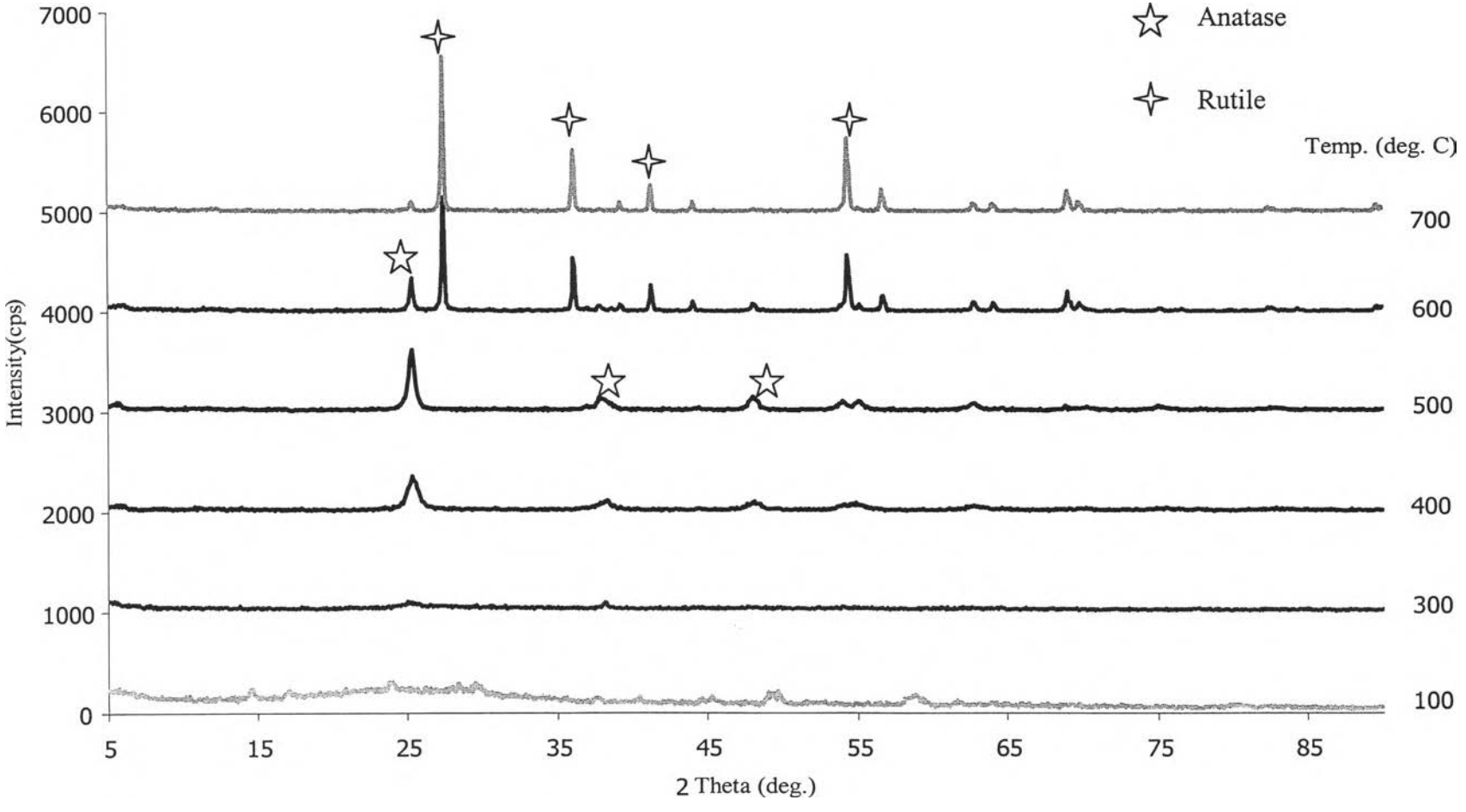

Figure 4.12 XRD patterns of titanium dioxide precipitated at different calcination temperature in w/o microemulsion containing 0.3 M $TiCl_4$ and 4.0% NaCl and precipitaed at pH 6.0.

4.2.1.3 Synthesis of titanium dioxide particles in different types of microemulsion

Precipitation of titanium dioxide synthesized in three different types of microemulsion calcined at 460°C for 5 hours was subjected to XRD analysis and the results of XRD patterns shown in Figure 4.13 were compared with the titanium dioxide reference (P25). The XRD pattern of P25 titanium dioxide showed anatase and rutile, while the titanium dioxide obtained from the three types of microemulsion was anatase.

Figure 4.14 shows XRD patterns of titanium dioxide synthesized in w/o microemulsion with various salt concentrations. All XRD patterns show mainly anatase phase. It also shows that the amount of anatase phase increases as the salt concentration increases. Table 4.1 shows calculation of the amount of rutile phase based on the area of anatase peak at 25.3 degree 2θ and rutile peak at 27.5 degree 2θ (Jung and Park, 1999). At 7.0 wt% NaCl and above, the peak of rutile phase could not be detected.

Table 4.1 Amount of rutile phase (%) calculated based on XRD data of anatase and rutile peak areas.

Samples	% NaCl	% Rutile
Commercial titanium dioxide (P25)	-	24.15
TiO_2 synthesized in w/o microemulsion	4.0	18.88
TiO_2 synthesized in w/o microemulsion	5.0	11.09
TiO_2 synthesized in w/o microemulsion	6.0	6.48
TiO_2 synthesized in w/o microemulsion	7.0	N/A
TiO_2 synthesized in w/o microemulsion	8.0	N/A

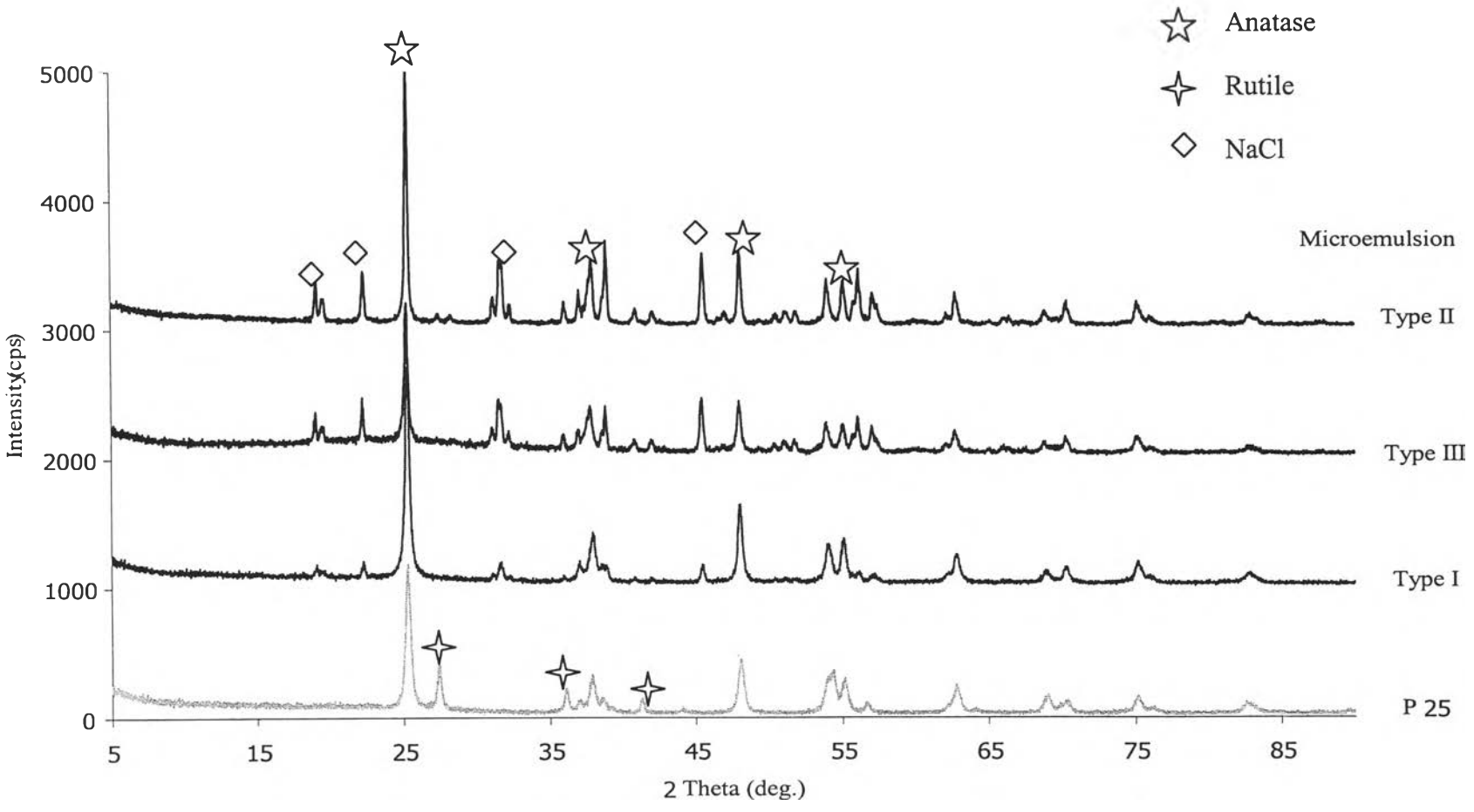

Figure 4.13 XRD patterns of titanium dioxide particles synthesized from different types of microemulsion, precipitated at pH 6.0 and calcined at temperature 460°C.

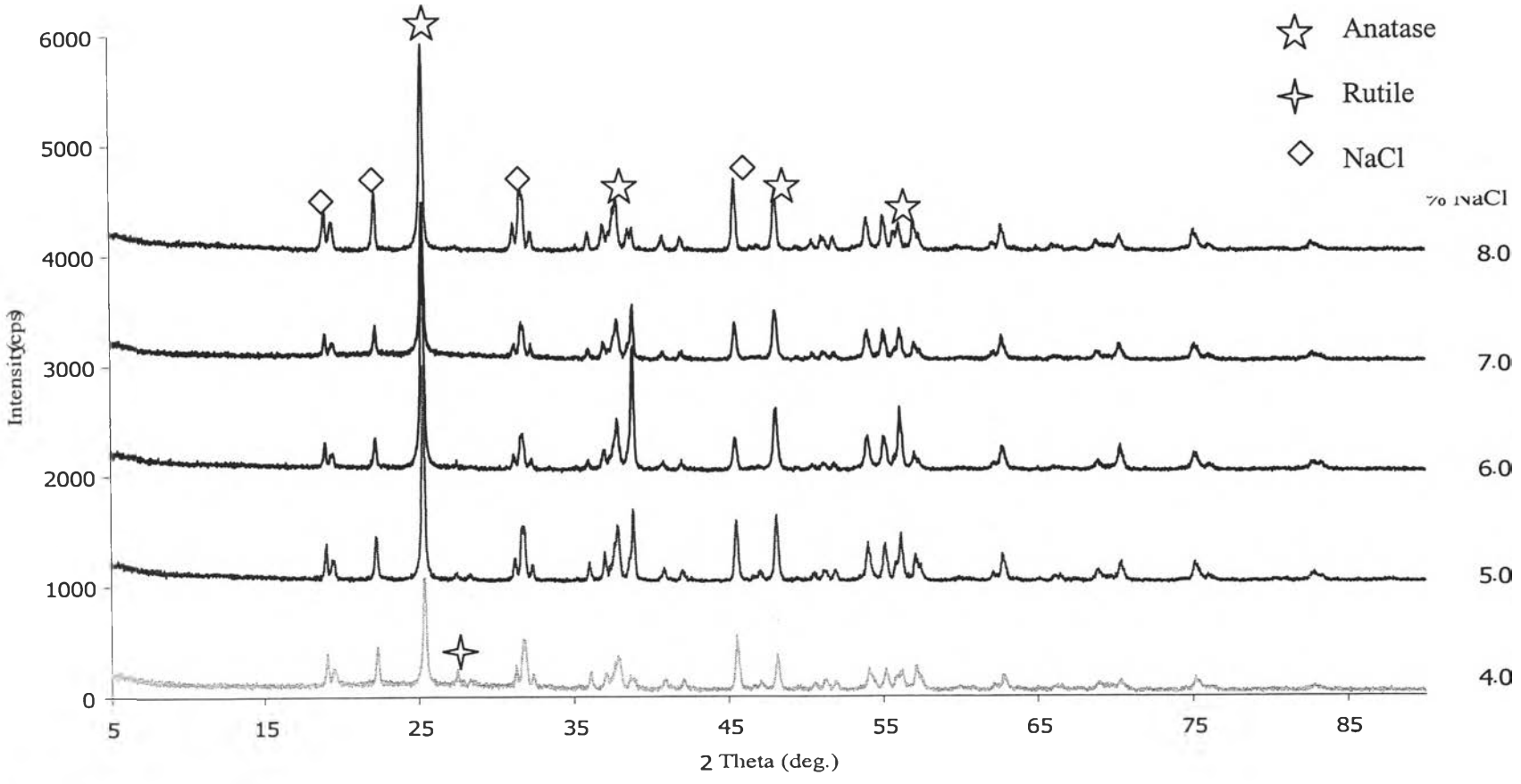

Figure 4.14 XRD patterns of titanium dioxide synthesized in w/o microemulsion with varying NaCl concentration and calcination temperature at 460°C.

The specific surface area of titanium dioxide nanoparticle decreased rapidly from 317.5 to 8.4 m^2/g with increasing the calcination temperature from 300 to 900°C (Kim and Hahn, 2001). This is due to the fact that the calcination temperature causes the agglomeration in nanoparticles and results in particles of bigger size and less surface area. The BET specific surface areas of titanium dioxide were determined and reported in Table 4.2. As the salt concentration increases, microemulsion structure changed from o/w to bicontinuous and to w/o. The titanium dioxide obtained from o/w microemulsion had approximate specific surface area, similar to the P25 titanium dioxide, while the particles obtained from bicontinuous microemulsion was higher, and w/o microemulsion was the highest specific surface area of samples prepared. Table 4.2 also shows that increasing the NaCl concentration from 0.4 to 8.0 wt% resulted in the increase in specific surface area of TiO_2 from 51.23 to 519.40 m^2/g and pore volume of TiO_2 from 1.33×10^{-7} to 4.24×10^{-7} m^3/g, but decrease in pore radius of TiO_2 from 31.81 to 28.47 nm.

Figure 4.15 (a) to (f) shows SEM results of TiO_2 obtained from four different synthesizes. SEM image of TiO_2 synthesized in o/w microemulsion (b) shows agglomerate of the primary nanoparticle similar to the P25 commercial titanium dioxide (a). The SEM image of titanium dioxide synthesized in bicontinuous microemulsion (c) shows less agglomeration while that of TiO_2 synthesized in w/o microemulsion (d) to (f) shows monodispersion in size of nanoparticle and does not have the agglomeration.

Table 4.2 Specific surface area, pore volume, and pore radius of titanium dioxide particle synthesized from different types of microemulsion and commercial titanium dioxide.

Samples	%NaCl	Surface area (m^2/g)	Pore volume (10^{-7} m^3/g)	Pore radius (nm)
Commercial titanium dioxide (P25)	-	58.36	0.92	32.02
TiO_2 synthesized in o/w microemulsion	0.4	51.23	1.33	31.81
TiO_2 synthesized in microemulsion type III	2.0	89.85	1.71	31.74
TiO_2 synthesized in w/o microemulsion	4.0	168.30	1.79	31.37
TiO_2 synthesized in w/o microemulsion	5.0	282.20	1.88	30.73
TiO_2 synthesized in w/o microemulsion	6.0	402.40	2.43	30.24
TiO_2 synthesized in w/o microemulsion	7.0	493.20	3.23	29.14
TiO_2 synthesized in w/o microemulsion	8.0	519.40	4.24	28.47

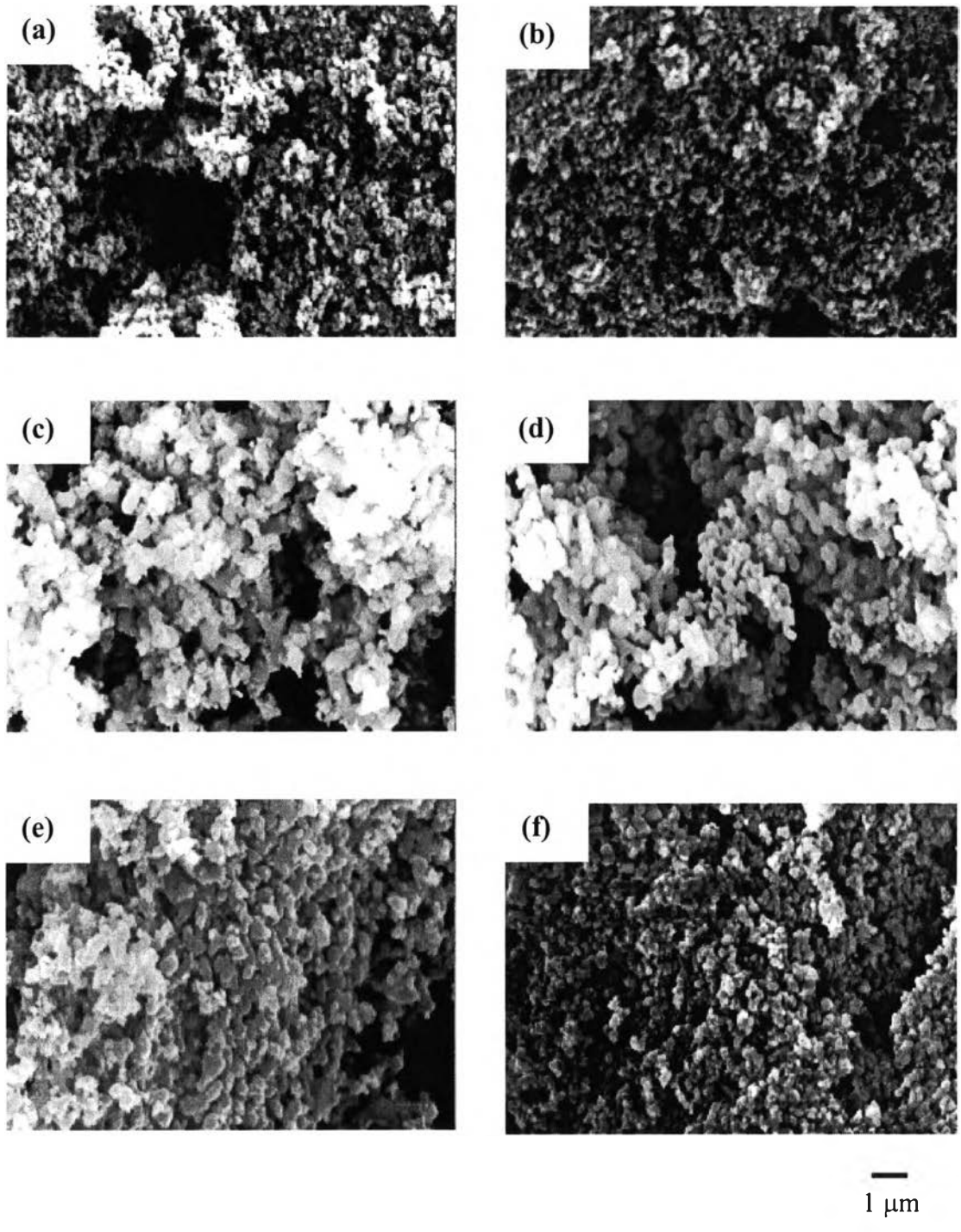

Figure 4.15 Scanning electron microscope of titanium dioxide obtained from (a) P25 commercial titanium dioxide, (b) o/w microemulsion (0.4% NaCl), (c) bicontinuous microemulsion (2.0% NaCl), (d) w/o microemulsion (4.0% NaCl), (e) w/o microemulsion (6.0% NaCl), and (f) w/o microemulsion (8.0% NaCl).

4.2.1.4 Size estimation

The particle size of titanium dioxide can be calculated using Debye-Scherrer equation and XRD data based on the data of anatase peak at 25.3 degree 2θ (Jung and Park, 1999; Chhabra *et al.*, 1995). In addition, the particle size was determined by dynamic light scattering using dilute TiO_2 in acetone. The results are reported in Table 4.3. The particle size of titanium dioxide obtained from o/w microemulsion (0.4 %NaCl) was similar to those results of P25. At 2.0 %NaCl, the titanium dioxide particles obtained from bicontinuous microemulsion have different particle sizes, which may imply polydispersion in particle size. Increasing the salt concentration resulted in the decrease of the particle size of titanium dioxide obtained from w/o microemulsion. Both methods are found to be in agreement with those observed in the TEM reported.

Figure 4.16 shows TEM results of four different titanium dioxide nanoparticles in comparison with P25 commercial titanium dioxide. The P25 titanium dioxide as shown in Figure 4.16 (a) has an average diameter of 30 nm while the synthesized in o/w microemulsion as shown in Figure 4.16 (b) is 33 nm in size. Titanium dioxide obtained from both o/w microemulsion and P25 contained both anatase and rutile. TEM micrographs of the titanium dioxide nanoparticle synthesized in bicontinuous microemulsion are shown in Figure 4.16 (d). It shows a polydisperse sample with average particle size of 66 nm. The micrograph of titanium dioxide particles synthesized in w/o microemulsion (Figure 4.16 (c) to (f)) indicated that these titanium dioxide particles were anatase, monodispersed, and very high crystallinity. The average particle size is decreased from 33 nm to 13 nm as NaCl concentration increases from 4.0 to 8.0 %.

Table 4.3 Comparison of particle size of titanium dioxide (nm).

Samples	TEM	XRD	DLS
P25	30.00	38.43	38.03
0.4% NaCl	33.30	32.02	56.50
2.0% NaCl	66.70	38.43	73.77
4.0% NaCl	36.70	32.03	39.23
5.0% NaCl	33.30	29.56	33.57
6.0% NaCl	26.70	25.20	27.96
7.0% NaCl	20.00	19.22	19.83
8.0% NaCl	13.30	14.78	13.35

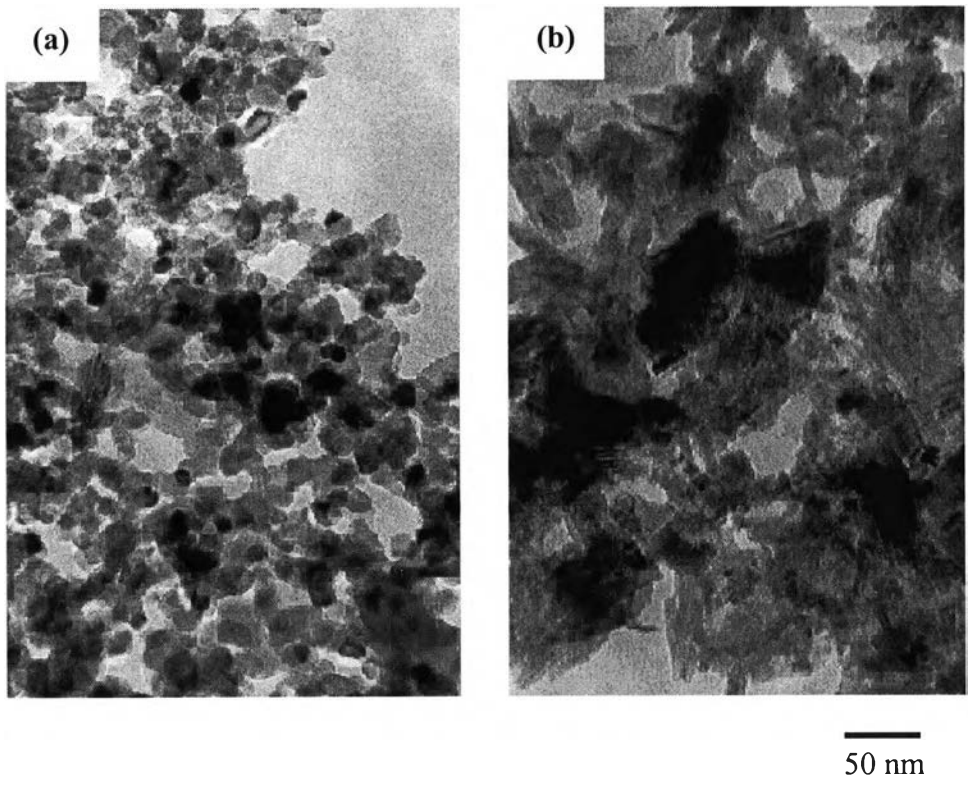

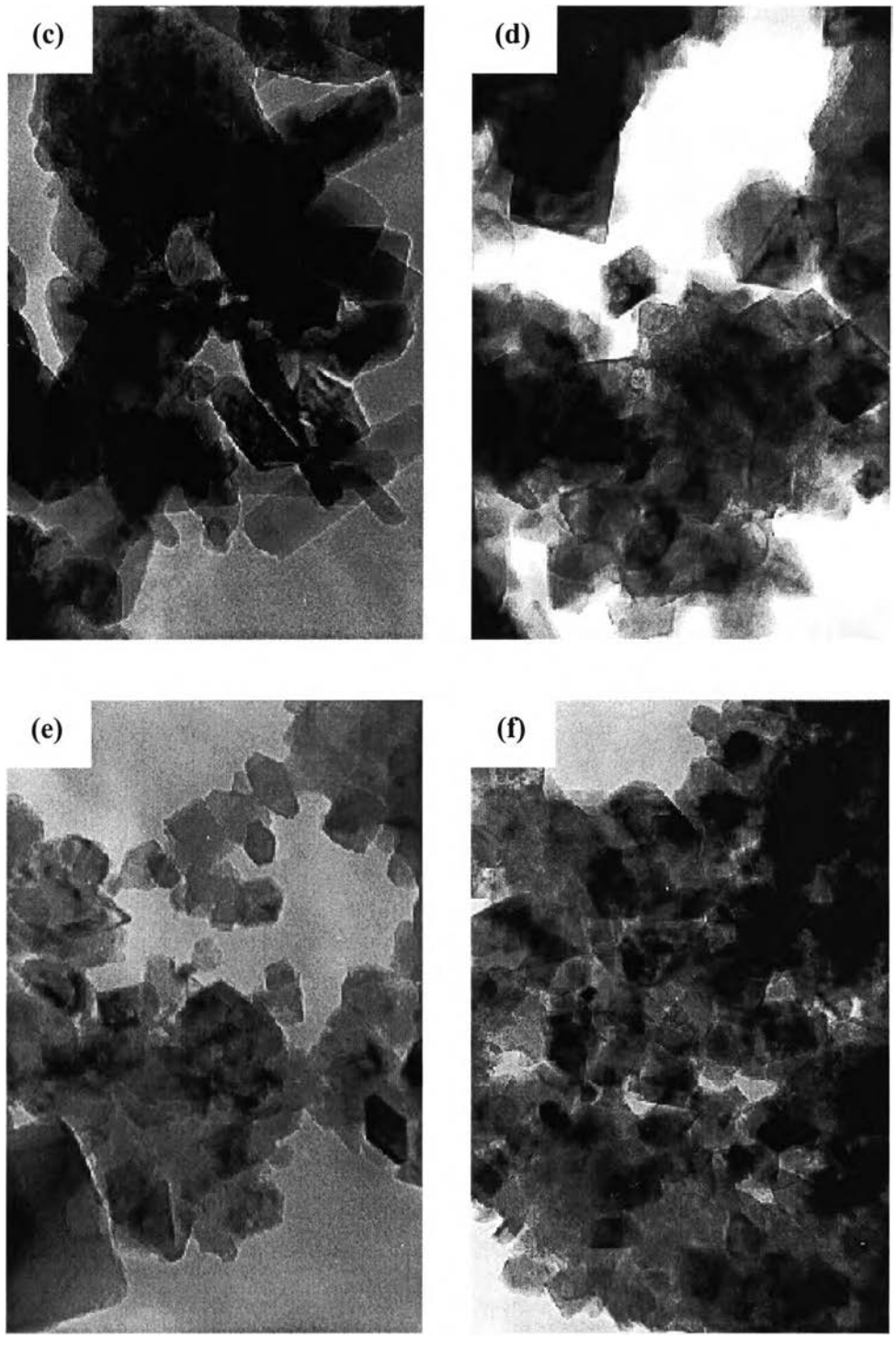

Figure 4.16 Transmission electron microscope of titanium dioxide obtained from (a) P25 commercial titanium dioxide, (b) 0.4% NaCl, (c) 2.0% NaCl, (d) 4.0% NaCl, (e) 6.0% NaCl, and (f) 8.0% NaCl. (——— 50 nm)